

СООБЩЕНИЯ  
ОБЪЕДИНЕННОГО  
ИНСТИТУТА  
ЯДЕРНЫХ  
ИССЛЕДОВАНИЙ

Дубна

98-385

E11-98-385

A.S.Vodopianov, Yu.A.Shishov, M.B.Yuldasheva,  
O.I.Yuldashev

COMPUTER MODELS OF DIPOLE MAGNETS  
OF A SERIES «VULCAN»  
FOR THE ALICE EXPERIMENT

1998

## Introduction

A big solenoidal magnet L3, a muon filter and a dipole magnet are the basic elements of the spectrometer magnetic system for the ALICE experiment. Fig.1 gives the 1/2 symmetrical part of the geometrical model of the spectrometer magnetic system with a superconducting dipole magnet. The papers [2,3,4,5] are devoted to the development of projects for the dipole magnet. The main requirements on the projected dipole are conditions on integrals of the field component, that is orthogonal to the beam axis. The desired economy when manufacturing and exploiting the dipole magnet have led to the development of a series of projects named as "VULCAN". All the projects have been developed in JINR and were used as a base for the magnet in [5]. Geometrical models of the magnets of the series are presented in fig.2. Their typical feature is that all the magnets are "warm" and their coils are of conic saddle shape.

The paper suggests a construction algorithm of a computer model for such a coil. The coil field is computed by the Biot-Savart's law. In this connection some integrals are successfully calculated by means of analytical formulas.

The computer models for the "VULCAN" magnets have been constructed in the framework of a differential approach for two scalar potentials  $\xi$ ,  $\eta$ , which are introduced by formulas [6]:  $\vec{H} = -\nabla\xi$  in the magnetic material and  $\vec{H} = -\nabla\eta + \vec{H}^*$  exterior to the magnetic material. Here  $\vec{H}$  is the magnetic field intensity, vector  $\vec{H}^*$  is computed by the Biot-Savart's law. These methods were described in detail in [7,8,9]. They are based on solving a boundary-value problem for two scalar potentials  $\xi$  and  $\eta$  by means of the finite element method (FEM):

$$\begin{aligned} \nabla \cdot (\mu \nabla \xi) &= 0 && \text{in the magnetic material,} \\ \nabla \cdot \nabla \eta &= 0 && \text{exterior to the magnetic material,} \end{aligned}$$

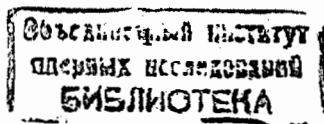
with the following conditions on the boundary between two mediums

$$\mu(\partial\xi/\partial n) = \partial\eta/\partial n - \vec{n} \cdot \vec{H}^*, \quad \xi = \eta + \eta^*,$$

and the condition  $\eta = 0$  on a boundary that is distant enough from the magnetic material. Function  $\mu = \mu(|\nabla\xi|)$  is known, potential  $\eta^*$  is defined by formula

$$\eta^*(P) = \eta^*(Q) - \int_Q^P H_r^* dt.$$

On the next stage, the modeling has been performed with regard to a local accuracy control of computations. Here in parallel with the already known algorithm, two new algorithms are used. The former is based on a comparison of the fields computed by means of linear and square base functions. The latter is based on the definition of the local classical solution to the problem for FEM.



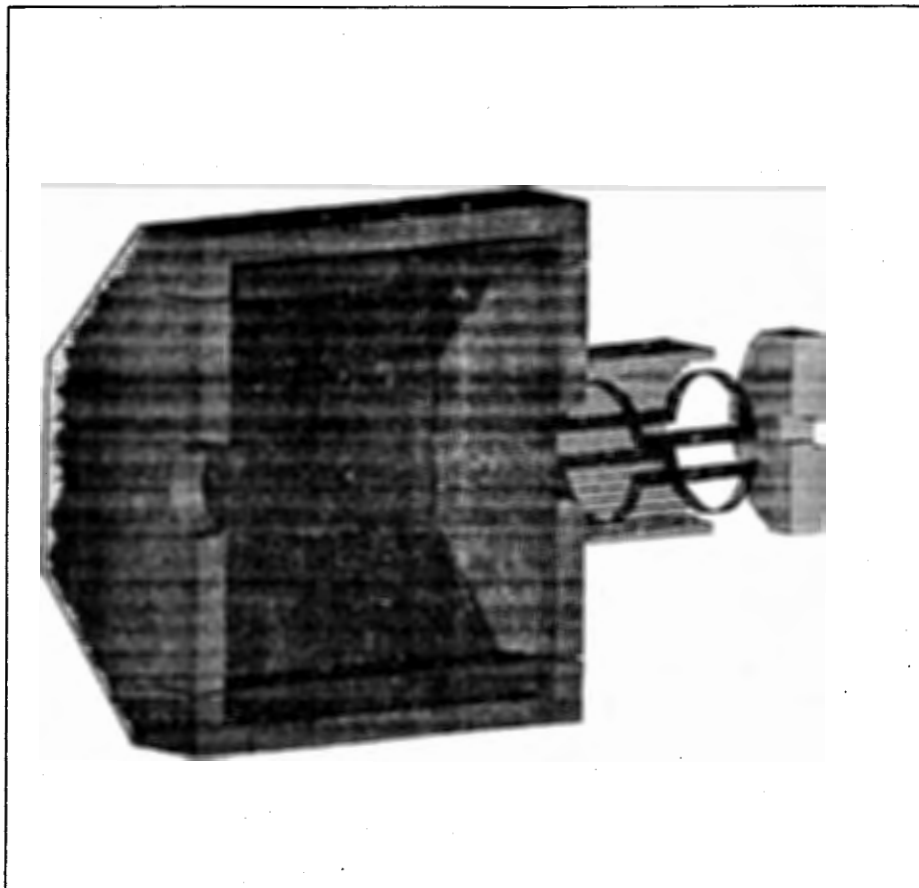
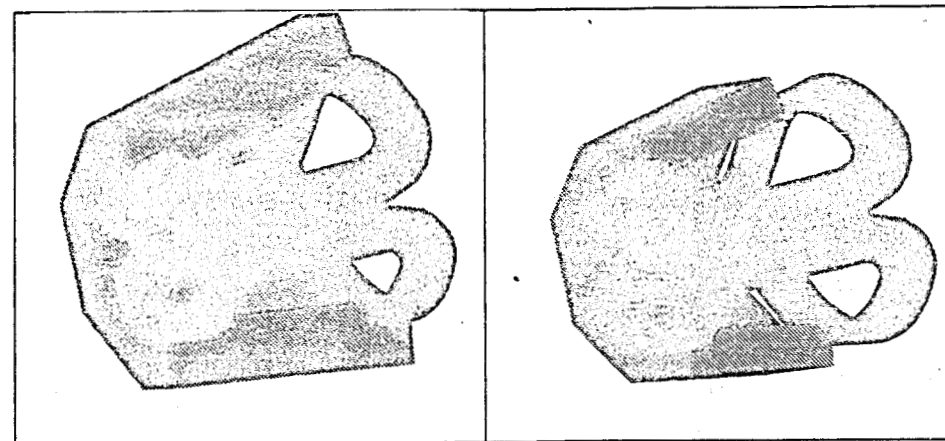
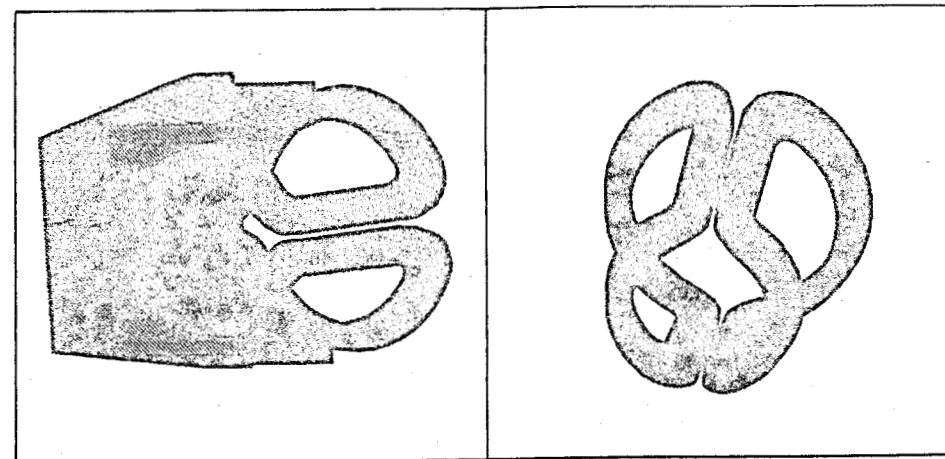


Fig.1. The magnetic system of the spectrometer ALICE, containing solenoidal magnet L3, superconducting dipole magnet and muon filter (the 1/2 symmetrical part is represented).



a)

b)



c)

d)

Fig.2. Models of magnets from the "VULCAN" series (the 1/2 symmetrical part is shown): a), b), c) - the first, second and third magnets; d) - the coil of the third magnet.

# 1 Construction of computer models for the coils

The magnetic field intensity exterior to the magnetic material can be conveniently represented as a sum

$$\vec{H} = \vec{H}^J + \vec{H}^s, \quad (1)$$

where vector  $\vec{H}^J = -\nabla\eta$  is a contribution of the ferromagnetic material, and vector  $\vec{H}^s$  is the coil field intensity computed by the Biot-Savart's law:

$$\vec{H}^s(P) = \frac{1}{4\pi} \int_{\Omega_s} \vec{J} \times \nabla \frac{1}{R_{PQ}} d\Omega_Q, \quad (2)$$

where  $\Omega_s$  is a coil region,  $\vec{J}$  is a known vector of the current density,  $R_{PQ}$  is the distance between points  $P$  and  $Q$ .

Note that  $\vec{H}^s$  is a classical solution of the following equations

$$\nabla \cdot \vec{H}^s = 0, \quad \nabla \times \vec{H}^s = 0, \quad \lim_{P \rightarrow \infty} \vec{H}^s(P) = 0,$$

within the whole space excepting the region  $\Omega_s$ . Here

$$\nabla \cdot \vec{H}^s = 0, \quad \nabla \times \vec{H}^s = \vec{J}.$$

For the computation of the integrals in (2), we suggest the following. Let the coil be located on a lateral area of straight frustum of a cone. In a space with Cartesian coordinate system  $(x, y, z)$  such a cone may be characterized by the inclination angle of the generator  $\alpha$  and  $z$ -coordinate of the vertex  $z_c$ . Let  $L$  be a length of the generator and  $\psi$  be an angle value on the lateral area of a cone (fig.3). Then we obtain:

$$\begin{aligned} x &= r \cdot \sin\varphi' = L \cdot \sin\alpha \cdot \sin(\psi/\sin\alpha), \\ y &= r \cdot \cos\varphi' = L \cdot \sin\alpha \cdot \cos(\psi/\sin\alpha), \\ z &= z_c + L \cdot \cos\alpha. \end{aligned} \quad (3)$$

Thus, the location of a point on the lateral area of the cone is characterized by the couple of variables  $(L, \psi)$ . The evolvent of the lateral area of the coil is decomposed by the five types of superelements as it is shown in fig.3. The coil as the whole may be considered as a sequence of layers bounded by the lateral areas of the cones with the same inclination angles of the generator and the different  $z$ -coordinates of vertices. In this connection, an important condition is a conservation of a cross-section area of the coil and lengths of the arcs on the lateral areas of cones.

The method for calculating the integral (2) depends on a type of the integration region. For example, to compute the integrals over the volume formed by superelements of types 1 and 5, some analytical formulas for a double integration with a consequent numerical integration are used.

Let us present these formulas presupposing that in a cylindrical coordinate system  $\Omega_s = \{(r, \varphi, z) : r_1 \leq r \leq r_2, \varphi_1 \leq \varphi \leq \varphi_2, p_1 r + q_1 \leq z \leq p_2 r + q_2, p_k, q_k =$

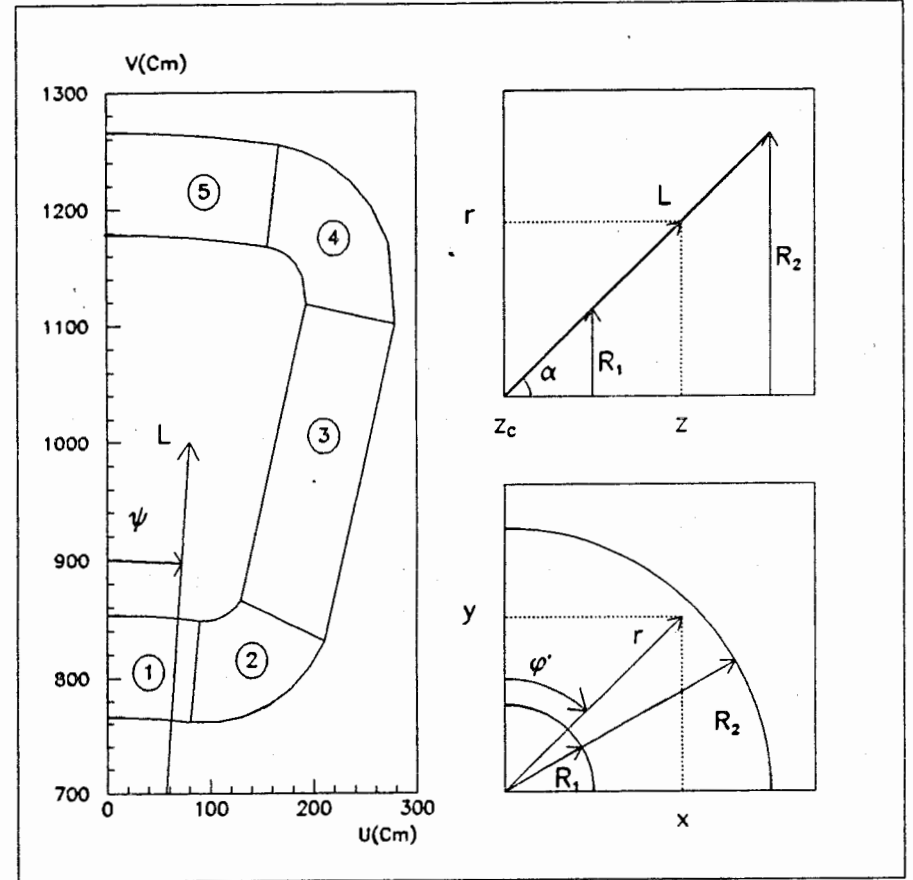


Fig.3. The quarter of evolvent of lateral area of frustum of a cone and parameters for the transformation (3).

$const \neq 0, k = 1, 2$ , i.e.  $\Omega$ , is a solid formed by rotating a triangle or a quadrangle around the axis  $oz$ . The analytical formulas for the region  $\Omega$ , obtained by the rotation of the rectangle with the sides parallel to the coordinate axes, are given in [10].

In our case the integral (2) takes the form

$$\vec{H}^*(r_0, \varphi_0, z_0) = \frac{J_0}{4\pi} \int_{\Omega} (z \cos(\theta) \vec{i} + z \sin(\theta) \vec{j} + (r - r_0 \cos(\theta)) \vec{k}) \frac{-r}{R^3} dz dr d\varphi,$$

where  $J_0$  is a current density,  $\theta = \varphi - \varphi_0$ ,  $R$  is a distance in the cylindrical coordinate system. After the double integration, we have for the first two vector components

$$\iint \frac{-zr}{R^3} dz dr = \frac{\rho}{a} - \frac{b}{a^{3/2}} \ln \left| \frac{ar + b}{\sqrt{a}} + \rho \right|,$$

where

$$\rho = \sqrt{ar^2 + 2br + c}, \quad a = p_k^2 + 1, \quad b = p_k(q_k - z_0) - r_0 \cos(\theta), \quad c = r_0^2 + (q_k - z_0)^2.$$

For the third vector component we have

$$\iint \frac{-(r - r_0 \cos(\theta))r}{R^3} dz dr = \frac{\rho}{a} + \frac{1}{\sqrt{a}} \left( s - \frac{b}{a} \right) \ln \left| \frac{ar + b}{\sqrt{a}} + \rho \right| +$$

$$+ \operatorname{sgn}(s) r_0 \cos \theta \ln \sqrt{|G_1|} + r_0 |\sin \theta| \operatorname{arctg} G_2,$$

where

$$s = p_k r_0 \cos \theta + q_k - z_0,$$

$$G_1 = \frac{\rho - \operatorname{sgn}(s)(p_k r + q_k - z_0)}{\rho + \operatorname{sgn}(s)(p_k r + q_k - z_0)}, \quad G_2 = \frac{p_k r_0^2 \sin^2 \theta - (r - r_0 \cos \theta)s}{r_0 |\sin \theta| \rho}.$$

Then the obtained formulas are used for a numerical integration over the variable  $\varphi$ .

To compute integrals over the volumes formed by superelements of types 2 and 4, the Gaussian cubature formulas for cube [11] are used.

The volume formed by superelements of type 3 is divided into two parts. The double integration with the above-mentioned analytical formulas is realized for the first one and the Gaussian cubature formulas are used for the second part.

## 2 Construction of computer models for the magnets under the local accuracy control

For the magnetic field modeling of the "VULCAN" magnets the code MSFE3D [7] is used. Due to a symmetry of the magnets it is enough to solve the boundary-value problem in the 1/4 part of space. The conditions  $\vec{B} \cdot \vec{n} = 0$  and  $\vec{B} \times \vec{n} = 0$  are used, respectively, on the vertical and horizontal planes of the symmetry. Figs. 4a)-4c) show the partition of the magnet calculating region by hexahedronal elements.

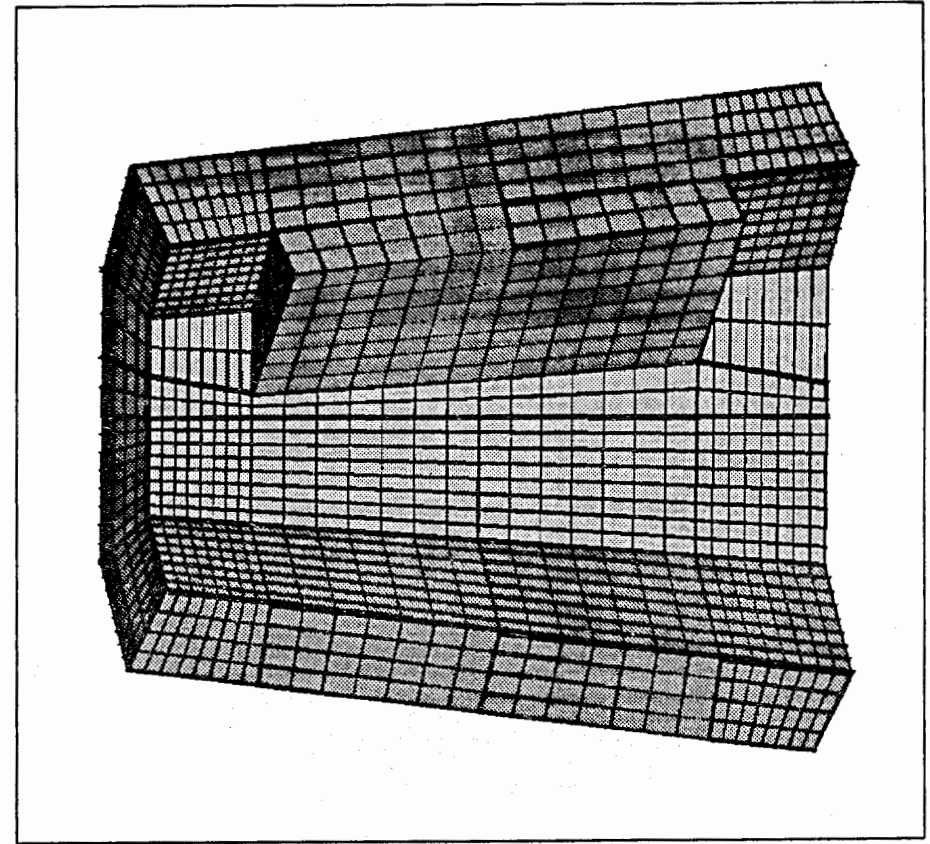


Fig.4a. The partition of the first magnet calculating region by elements.

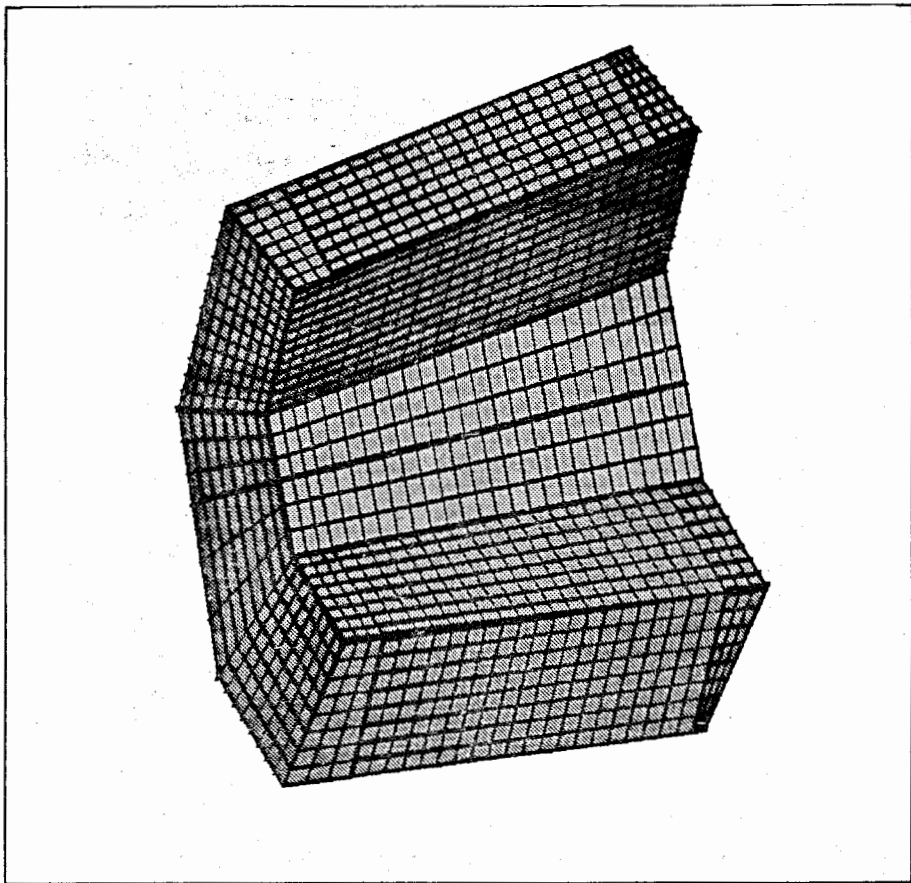


Fig.4b. The partition of the second magnet calculating region by elements.

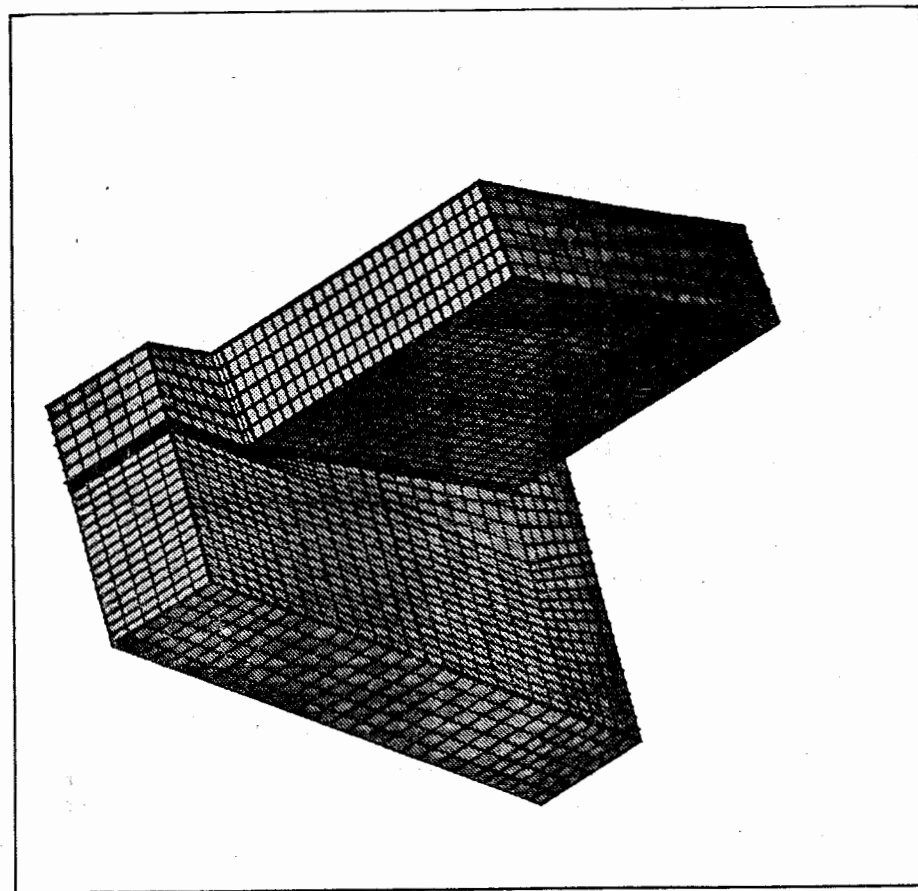


Fig.4c. The partition of the third magnet calculating region by elements.

Several approaches exist to create the procedures for a local accuracy control when solving magnetostatic problems by FEM (for example, see [12]). Note, that the accuracy must be higher, if the contribution of the coil field is larger. It is true for all these approaches when the summands in representation (1) have the same sign.

Let us select two most simple in realization and effective enough approaches. The continuity property of the normal component of the flux density vector and the tangential component of the field intensity vector on the boundary between any regions is used in the first approach. We presuppose that as a result of a numerical solving of the problem, a field is obtained in every element of discretization of the calculating region. Let  $\Gamma_i$  be a boundary of the  $i$ -th element,  $\vec{B}_i, \vec{H}_i$  are field vectors in this element,  $\vec{B}_{iout}, \vec{H}_{iout}$  are field vectors in the neighboring elements which have a common boundary with the  $i$ -th element. Then for the estimation of the local accuracy in the  $i$ -th element we can use the values

$$\theta_{1,i}^n(\vec{B}) = \frac{1}{|\Omega_i|} \int_{\Gamma_i} |(\vec{B}_i - \vec{B}_{iout}) \cdot \vec{n}| d\Gamma, \quad (4)$$

$$\theta_{1,i}^t(\vec{H}) = \frac{1}{|\Omega_i|} \int_{\Gamma_i} |(\vec{H}_i - \vec{H}_{iout}) \times \vec{n}| d\Gamma, \quad (5)$$

where  $|\Omega_i|$  is a volume of the region  $\Omega_i$ ,  $\vec{n}$  is a vector of unit normal to the boundary  $\Gamma_i$ .

In the second approach two different methods of the field computation are used. Moreover, one of them gives a more correct result. To realize this approach, we prefer the following. Let us presuppose that the numerical solving of the problem gives the potentials  $\eta_j$ ,  $j = 1, 2, \dots, 8$  in vertices of the  $i$ -th hexahedral element, and let  $N_j^{(1)}$ ,  $j = 1, 2, \dots, 8$  be linear shape functions (for example, [13]). Then the magnetic field intensity created in this element by the magnetic material can be computed by the formula

$$\vec{H}^{J,1}(P) = - \sum_{j=1}^8 \eta_j \nabla N_j^{(1)}(P).$$

On the other hand, it is possible to construct a quadratic element, containing the  $i$ -th linear element and seven neighboring linear elements in the limits of every superelement with the sufficient number of partitions. Let the quadratic shape functions  $N_l^{(2)}$ ,  $l = 1, 2, \dots, 27$  be defined in this quadratic element. Then the vector  $\vec{H}^J$  can be computed by the formula

$$\vec{H}^{J,2}(P) = - \sum_{l=1}^{27} \eta_l \nabla N_l^{(2)}(P).$$

Thus, the accuracy of the field calculation in the element  $\Omega_i$  is characterized by the following value

$$\theta_{2,i}(\vec{H}) = \frac{1}{|\Omega_i|} \int_{\Omega_i} |\vec{H}^{J,1} - \vec{H}^{J,2}| d\Omega. \quad (6)$$

It is necessary to note that when solving the magnetostatic problems by FEM with first- or second- order base functions, the obtained solution is not classical in view of a insufficient smoothness of the generalized functions [14]. Therefore, it is possible to obtain "semi-classical" solutions only using the representation (1) and the above-mentioned formulas for a computation of the magnetic field intensity  $\vec{H}^J$ .

However, it is naturally to require that the magnetic field has continuous partial derivatives and the following equations are true

$$\nabla \cdot \vec{H}^J = 0, \quad \nabla \times \vec{H}^J = 0$$

in some quite extensive and interesting for us region  $\bar{\Omega}$ , i.e. the field is locally classical. If on a boundary of the region  $\bar{\Omega}$  the vector  $\vec{H}^J$  is known, then the problem of the required field finding has a unique solution [15],[16] and it is represented in the following form

$$\vec{H}^{J,c}(P) = \frac{\nabla}{4\pi} \int_{\Gamma} \frac{\vec{H}^J \cdot \vec{n}}{R_{PQ}} d\Gamma_Q - \frac{\nabla \times}{4\pi} \int_{\Gamma} \frac{\vec{H}^J \times \vec{n}}{R_{PQ}} d\Gamma_Q, \quad (7)$$

where  $\bar{\Gamma}$  is a boundary of the region  $\bar{\Omega}$ . To recalculate the magnetic field intensity  $\vec{H}^J$  by the formula (7), it is naturally to define the characteristic

$$\theta_{3,i}(\vec{H}) = \frac{1}{|\Omega_i|} \int_{\Omega_i} |\vec{H}^{J,1} - \vec{H}^{J,c}| d\Omega \quad (8)$$

in every element  $\Omega_i$ , belonging to the region  $\bar{\Omega}$ .

The characteristics (6) and (8) are used for the local accuracy control.

### 3 Computed results

According to conditions of the experiment, the dipole magnet of the spectrometer ALICE must satisfy the requirements [1]: the integral of the main field component is equal to  $3 T \cdot m$ , the field magnitude in the centre of the magnet is  $0,7 T$ , the diameter of the free aperture is  $3,9 m$ , its length  $L_m \approx 5 m$ . In view of this, we give the values of the parameters for all three magnets of series "VULCAN". Table 1 presents the maximal field magnitudes  $B_m$  on the axes of the magnets, the current densities in the coils, the areas of the coil cross-sections  $S$ , the diameters of free apertures  $D$  and the lengths of the magnets  $L_m$ . Table 2 gives the integrals of the main field component within the magnet aperture. The integrand is computed in the polar coordinate system  $(r, \theta, \varphi)$  on the rays starting from the point that approximately corresponds to the centre of the magnet L3.

Fig.5 shows the behaviour of the field component  $B_y$  along these rays for all three magnets for  $\varphi = 45^\circ$ . The point with coordinates  $x = y = z = 0$  corresponds to the centre of the magnet.

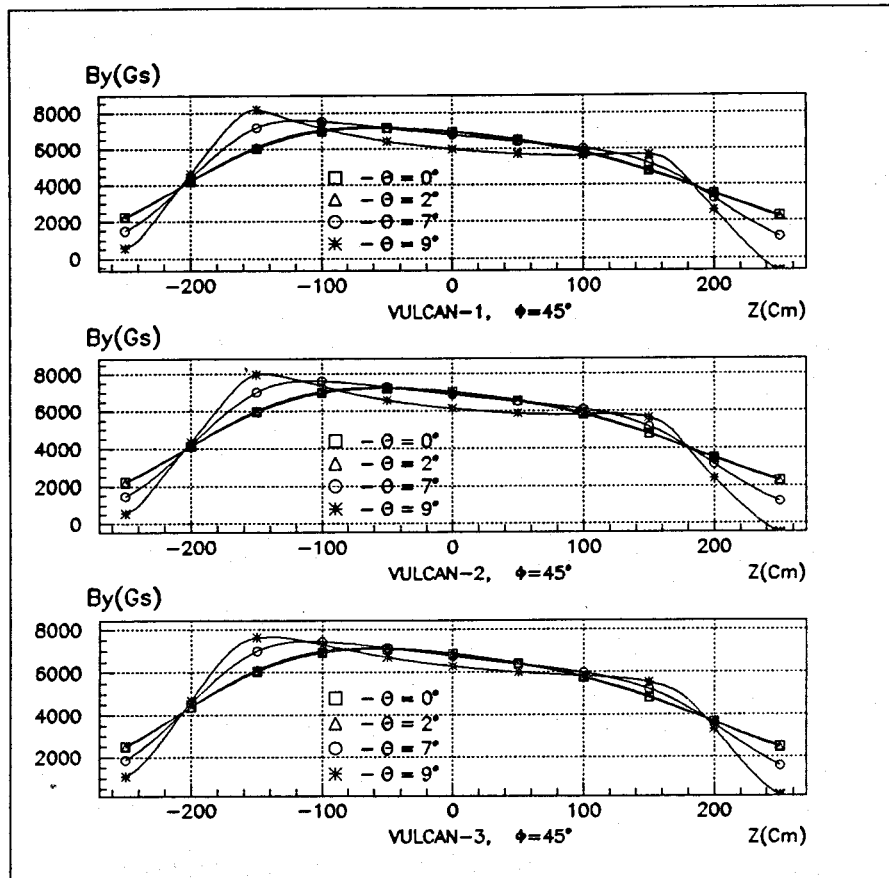


Fig.5. The behaviour of main field component along rays in polar coordinate system for three magnets.

The accuracy of the field computations can be characterized, to a certain degree, by the local accuracy estimations obtained in some part of the magnet aperture. The third magnet and the part of its aperture, contained in the volume  $V = \{(x, y, z) : |x| \leq 2m, |y| \leq 1m, |z| \leq 1m\}$  are considered as an example. Table 3 presents the maximal and the minimal values of the characteristics (4),(5),(6),(8) for the obtained flux density vector with respect to the maximal field magnitude  $B_m$  on the magnet axis:

$$\theta_{1,i}(\vec{B}) = \theta_{1,i}^n(\vec{B}) + \theta_{1,i}^t(\vec{B}), \quad \theta_{2,i}(\vec{B}), \quad \theta_{3,i}(\vec{B}). \quad (9)$$

Note that the coil field contribution is equal to 58.8 % in the point of the magnet axis, where the maximal field magnitude  $B_m$  is reached.

Table 1

number of magnet	$B_m(T)$	current density ( $A/cm^2$ )	$S(m^2)$	$D(m)$	length $L_m(m)$
1	0.7145	242.	0.35	2.42-4.	5.
2	0.7212	242.	0.35	2.42-4.	5.
3	0.7089.	241.21	0.3918	2.58-4.1	5.

Table 2

number of magnet	$\int_{L_m} B_y dl (T \cdot m)$				
		$\theta = 0^\circ$	$\theta = 2^\circ$	$\theta = 7^\circ$	$\theta = 9^\circ$
1	$\varphi = 0^\circ$	2.712	2.749	3.217	3.456
	$\varphi = 45^\circ$	2.712	2.728	2.792	2.636
	$\varphi = 90^\circ$	2.712	2.710	2.811	3.000
2	$\varphi = 0^\circ$	2.717	2.754	3.234	3.495
	$\varphi = 45^\circ$	2.717	2.733	2.795	2.647
	$\varphi = 90^\circ$	2.717	2.713	2.781	2.940
3	$\varphi = 0^\circ$	2.732	2.757	3.148	3.461
	$\varphi = 45^\circ$	2.732	2.748	2.823	2.749
	$\varphi = 90^\circ$	2.732	2.741	2.938	3.164

Figs. 6a)-6c)<sup>1</sup> give the behaviour of the relative characteristics (9) on the boundaries of considered volume  $V$  in the third magnet aperture. The value of every

<sup>1</sup>Color figures can be find in directory /afs/cern.ch/user/y/yuldash/public

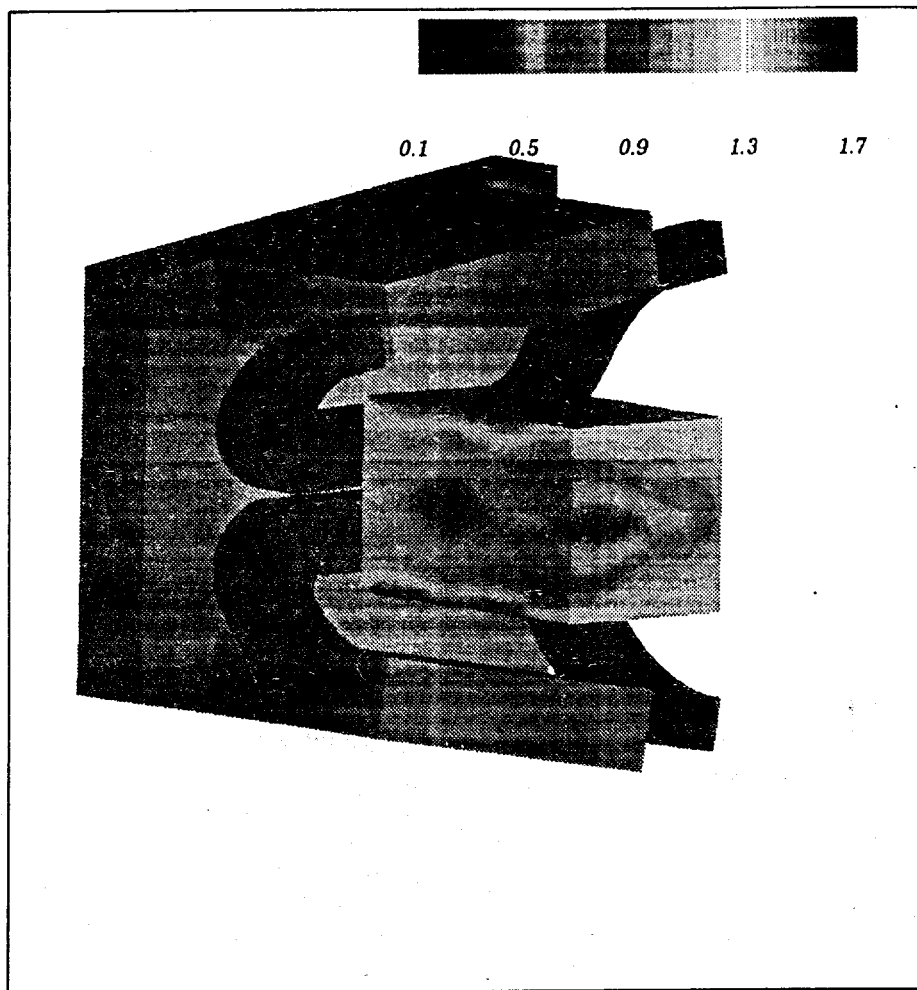


Fig.6a. The distribution of the characteristic  $\theta_1$  within middle part of the third magnet aperture.

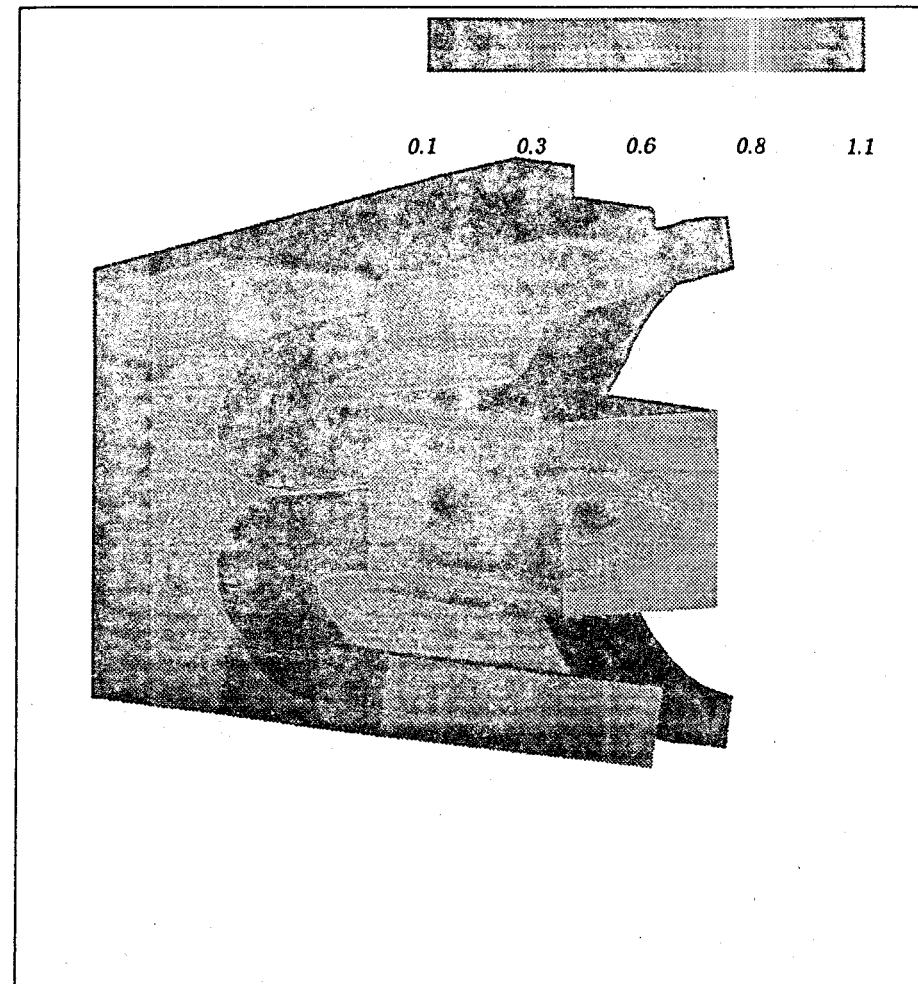


Fig.6b. The distribution of the characteristic  $\theta_2$  within middle part of the third magnet aperture.

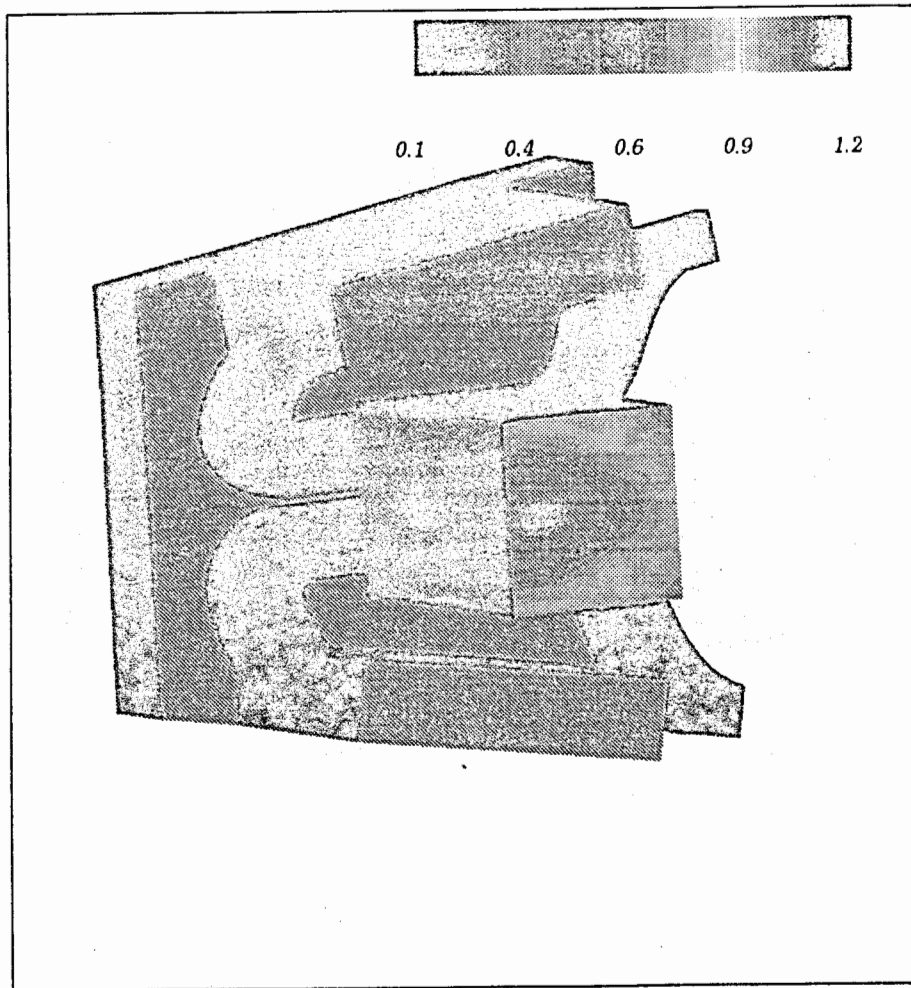


Fig.6c. The distribution of the characteristic  $\theta_3$  within middle part of the third magnet aperture.

characteristics with the number  $i$  corresponds to the centre of the  $i$ -th element. Every element in the volume  $V$  has the following dimensions:  $h_x = 10\text{cm}$ ,  $h_y = 8.3125\text{cm}$ ,  $h_z \approx 19.83\text{cm}$  ( $z < 0$ ),  $h_z \approx 20.875\text{cm}$  ( $z > 0$ ). As it is clear from these figures, the values of characteristics  $\theta_1(\vec{B})$ ,  $\theta_2(\vec{B})$ ,  $\theta_3(\vec{B})$  do not exceed 1.7, 1.1 and 1.2 %, respectively.

Table 3

$\theta_{1,i}(\vec{B})$ (%)		$\theta_{2,i}(\vec{B})$ (%)		$\theta_{3,i}(\vec{B})$ (%)	
min	max	min	max	min	max
0.11	1.66	0.064	1.10	0.084	1.20

**Acknowledgments.** The authors wish to express their gratitude to Prof. I.V.Puzynin for his encouragement of the work, Dr. P.G.Akishin for his fruitful collaboration as well as Dr. T.A.Strizh and Dr. Zh.Zh.Musulmanbekov for the useful discussions of graphic packages. O.I.Yuldashev also thanks the Russian Foundation for Basic Research for its support (grant N 98-01-00190).

#### REFERENCES

1. ALICE Technical Proposal, CERN/LHCC 95-71, 1995; The Forward Muon Spectrometer of ALICE (Addendum to the ALICE technical proposal), CERN/LHCC 96-32, 1996.
2. P.G.Akishin, et al. Superconducting Dipole Magnet for ALICE Dimuon Arm Spectrometer (Conceptual Design Report). JINR rapid communication, N 1 ( 81 ), 1997, c. 81-94.
3. P.G.Akishin et al. Conceptual design of the warm dipole magnet for the ALICE forward muon spectrometer. ALICE/96-26, Internal Note/MAG, 1996.
4. W.Flegel, D.Swoboda. A Warm Magnet for the ALICE Muon Arm. ALICE/96-24, Internal Note/MAG, 1996.
5. Preliminary Design Report for the Dipole Magnet of the Muon Spectrometer. ALICE Collaboration, Dipole Magnet Project Working Group. ALICE/98-07, Internal Note/MAG, 1998.
6. J.Simkin, C.W.Trowbridge. Three dimensional non-linear electromagnetic field computations using scalar potentials. Proc. IEE, 1980, vol.127, Pt.B, N6, pp. 368-374.

7. M.B.Yuldasheva, O.I.Yuldashev. The program complex MSFE3D for computation of three-dimensional magnetic fields. Version 1.2, JINR, P11-94-202, Dubna, 1994 (in russian).
8. E.P.Zhidkov, M.B.Yuldasheva, O.I.Yuldashev. Vector algorithms for solving 3D nonlinear magnetostatics problems. Mathematical modeling, v.6, N9, pp. 99-116, 1994 (in russian).
9. E.P.Zhidkov, M.B.Yuldasheva, I.P.Yudin, O.I.Yuldashev. Computation of the magnetic field of a spectrometer in detectors region. Nuclear Instruments and Methods-"A", 365 (1995), pp.308-316.
10. M.Gyimesi et al. Biot-Savart Integration for Bars and Arcs. IEEE Trans. on Mag., v.29, N 6, 1993, pp.2389-2391.
11. I.P.Mysovskih. Interpolational cubature formulas. M., "Nauka", 1981 (in russian).
12. Computational Magnetism (ed. J.K.Sykulski), London, "Chapman&Hall", 1995, pp. 305-312.
13. O.Zenkevich, K.Morgan. Finite elements and approximation., M., Mir, 1986 (in russian).
14. V.P.Mihailov. Differential equations in partial derivatives. M., "Nauka", 1976, p. 154 (in russian).
15. M.J.Friedman. Mathematical Study of the Nonlinear Singular Integral Magnetic Field Equation. Part I. SIAM J. Appl. Math., v.39, N 1, 1980, pp.15-17.
16. M.J.Friedman, J.E.Pasciak. Spectral Properties for the Magnetization Integral Operator. Mathematics of Computation, v.43, N 168, 1984, pp.447-453.

Received by Publishing Department  
on December 29, 1998.